Letter

Finite-temperature topological invariant for higher-order topological insulators

Congwei Lu,[1,2,3] Lixiong Wu,[1,3] and Qing Ai[1,3,*]

[1]*School of Physics and Astronomy, Applied Optics Beijing Area Major Laboratory, Beijing Normal University, Beijing 100875, China*

[2]*Department of Physics, Hong Kong Baptist University, Kowloon Tong, Hong Kong, China*

[3]*Key Laboratory of Multiscale Spin Physics, Ministry of Education, Beijing Normal University, Beijing 100875, China*

(Received 1 August 2024; revised 23 March 2025; accepted 11 April 2025; published 1 May 2025)

We investigate the effects of temperature on higher-order topological insulators (HOTIs). The finite-temperature topological invariants for HOTIs can be constructed by generalizing the Resta's polarization for the ground state to the ensemble geometric phase (EGP) for the mixed states, [C.-E. Bardyn, L. Wawer, A. Altland, M. Fleischhauer, and S. Diehl, Phys. Rev. X **8**, 011035 (2018)]. The EGP is consistent with the Resta's polarization both at zero temperature and at finite temperatures in the thermodynamic limit. We find that the temperature can change the critical point and thus induce a phase transition from a topologically trivial phase to a nontrivial phase in a finite-size system, manifesting changes in the winding of the EGP.

DOI: 10.1103/PhysRevB.111.L201101

The phases of quantum matter can be characterized and classified by the topology of their ground states [1–4]. The topological properties of quantum phases, such as protected edge states and quantized particle transport, all originate from the topological invariants of the bulk state [5–9], which can only be defined in the ground state. Therefore, how to characterize the topology of the finite-temperature quantum states or even the nonequilibrium steady states of open quantum systems is an important issue [10–26]. Recently, it has been shown that the many-body Resta's polarization [27] defined in the ground state can be generalized to the phase of the expectation value of the polarization operator in the Gaussian mixed states of fermions in one dimension (1D), i.e., the ensemble geometric phase (EGP), which can be directly measured [28]. The winding of the EGP of mixed states upon cyclic-parameter variation yields a quantized topological invariant, which can be related to the quantized particle transport in an auxiliary system weakly coupled to the fermion chain [29]. The concept of an EGP can be generalized to higher-dimensional systems [30,31], interacting systems [32,33], critical systems [34], systems with time-reversal symmetry [35,36], and dissipative systems [37,38]. However, all these extensions are limited to first-order topological systems.

Recently, higher-order topological insulators (HOTIs) have attracted broad interest due to their unconventional bulk-boundary correspondence [39–64]. In higher-order topological phases, a d-dimensional nth-order ($n \geqslant 2$) topological system hosts topologically protected gapless states on its $(d-n)$-dimensional boundaries. Up to now, much effort has been devoted to understanding the effects of disorders [65–68], electron-electron interactions [69–71], and electron-phonon interactions [72] on higher-order topological phase transitions. Nevertheless, the finite-temperature effects on higher-order topological phase transitions have not yet been studied. One may wonder whether the EGP can be generalized to HOTIs? Does the temperature affect the higher-order topological phase transitions?

In this Letter, we propose a topological invariant to characterize the topology of HOTIs at finite temperatures, and thus it enables us to study the effects of the temperature on the higher-order topological phase transition. To be specific, we introduce the many-body Resta's polarization of the noninteracting fermionic Benalcazar-Bernevig-Hughes (BBH) model [73,74] at zero temperature and generalize it to the finite-temperature case, thereby constructing a higher-order EGP. We show that the higher-order EGP can restore the Resta's polarization at zero temperature, while at finite temperatures, the higher-order EGP is consistent with the Resta's polarization in the thermodynamic limit. The winding of the higher-order EGP is quantized and thus can be utilized to characterize the higher-order topological phase transition at finite temperatures. We find that the temperature can affect the critical point of a finite-size system and induce a topological phase transition from a topologically trivial phase to a topologically nontrivial phase. As the temperature continues to increase, the system is expected to transit from a topologically nontrivial phase to a trivial phase with completely mixed states.

Higher-order topological invariant for a noninteracting fermionic model. We consider a noninteracting fermionic BBH square-lattice model [40,41] with a staggered potential and periodic driving. As shown in Fig. 1(a), the Hamiltonian with $N \times N$ unit cells reads

$$\mathcal{H}_0 = -\sum_{\langle i,j\rangle} \lambda_{ij} \hat{a}_i^\dagger \hat{a}_j + \Delta \sum_{x,y=0}^{N-1} \sum_{\mu=1}^{4} (-1)^\mu \hat{n}_{x,y;\mu}, \quad (1)$$

where $\hat{a}_i^\dagger$ is a fermionic creation operator at site $i = (x, y; \mu)$, $x, y \in \{0, 1, \ldots, N-1\}$ are the positional coordinates of the unit cell, and $\mu \in \{1, 2, 3, 4\}$ labels the four sites in each unit cell. $\hat{n}_i = \hat{a}_i^\dagger \hat{a}_i$ denotes the fermion number operator. The nearest-neighbor-hopping energy λ_{ij} in the unit cell

*Contact author: aiqing@bnu.edu.cn

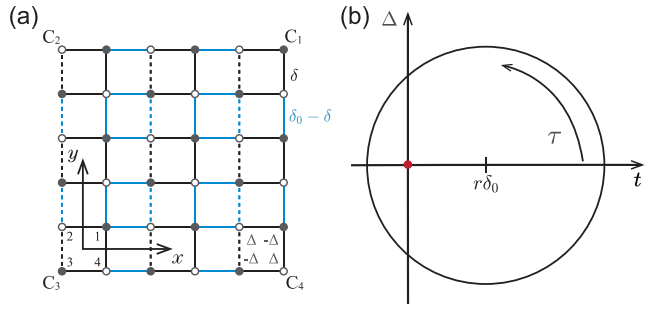

FIG. 1. (a) The square lattice of the BBH model with time-dependent nearest-neighbor intracell hopping constant $\pm\delta$, intercell hopping constant $\pm(\delta_0-\delta)$, and on-site potentials $\pm\Delta$. Solid lines take positive signs, while dashed lines take negative signs. (b) The pumping circle in parameter space (t,Δ). The arrow marks the evolution direction of the pump, and the red dot represents the gapless point of system.

and between two unit cells are respectively $\pm\delta$ and $\pm(\delta_0-\delta)$. $\pm\Delta$ are the staggered on-site potentials. The pump cycle is parametrized by $\tau\in[0,2\pi)$, with $t=(\delta_0-\delta)-\delta=\delta_0(\cos\tau+r)$ and $\Delta=\delta_0\sin\tau$, where $\delta=\delta_0(1-\cos\tau-r)/2$. As shown in Fig. 1(a), the solid lines take positive signs, while the dashed lines take negative signs. The undriven BBH model exhibits a second-order topological phase when $t>0$, featured by the appearance of in-gap localized states on the corners of the lattice [40,41]. The pumping circle with the center localized at $(t,\Delta)=(r\delta_0,0)$ in the parameter space (t,Δ) is shown in Fig. 1(b). When a pumping circle encloses the gapless point, i.e., $(t,\Delta)=(0,0)$, as shown in Fig. 1(b), the quantized charge will be transferred from the two antidiagonal corners to the two diagonal corners during an adiabatic cyclic evolution in half filling [75].

Now, we review the generalization of Resta polarization to the 2D hard-core Bose-Hubbard model as discussed in Ref. [75], and we apply it to the noninteracting fermion BBH model. Following Ref. [75], in order to investigate the charge-transport properties on higher-order corner states, we connect the four corners of the system to construct corner periodic boundary conditions (CPBCs), so that the current can pass through all four corners, and then study the total amount of charge Q_{c_2} flowing through corner c_2 during one pumping cycle.

The total bulk Hamiltonian with CPBC reads $\mathcal{H}^{\rm CPBC}=\mathcal{H}_0+\mathcal{H}^{\rm C}$, where the corner-connecting link Hamiltonian is

$$\mathcal{H}^{\rm C}=(\delta-\delta_0)\big(\hat{a}^\dagger_{c_2}\hat{a}_{c_1}+\hat{a}^\dagger_{c_1}\hat{a}_{c_4}+\hat{a}^\dagger_{c_4}\hat{a}_{c_3}-\hat{a}^\dagger_{c_3}\hat{a}_{c_2}\big)+\text{H.c.} \tag{2}$$

with corner sites $c_1=(N-1,N-1;1)$, $c_2=(0,N-1;2)$, $c_3=(0,0;3)$, and $c_4=(N-1,0;4)$. To construct topological invariants, we define the position operator under CPBC,

$$\hat{V}=\exp\left(i\frac{2\pi}{N}\hat{X}\right), \tag{3}$$

where

$$\hat{X}=\sum_{x\leqslant y}\sum_{\mu}(y-x)\hat{n}_{x,y;\mu}. \tag{4}$$

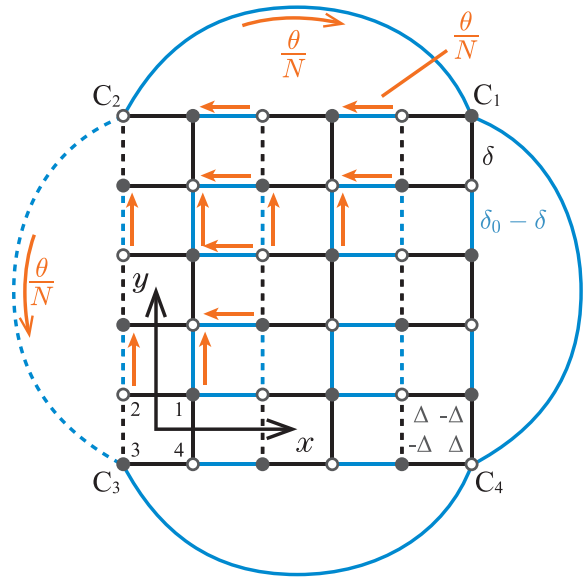

FIG. 2. The BBH model under CPBC with additional flux θ in the top and left supercells, and the net flux in each bulk plaquette is π. The orange arrows indicate that the hopping along the direction of the arrow needs to be multiplied by a phase factor $e^{i\theta/N}$.

The polarization P can be defined as

$$P=\frac{1}{2\pi}\text{Im}\ln\langle\psi_0|\hat{V}|\psi_0\rangle, \tag{5}$$

where $|\psi_0\rangle$ is the half-filling ground state of $\mathcal{H}^{\rm CPBC}$. Here, we only consider the electrons in the triangular region with vertices c_1, c_2, and c_3, whose polarization component along the diagonal direction is P. The polarization P is very important in our theory. First, it takes the form of the Zak phase. Second, its time derivative represents a physically meaningful current. Third, as we will see in the next section, P can be generalized to characterize the topology of the density matrix.

To explain that P is essentially the Zak phase, we first insert flux θ into two supercells near vertex c_2. We use the Peierls substitution and chose the gauge shown in Fig. 2. The corresponding Hamiltonian with flux θ is denoted as $\mathcal{H}^{\rm C}_V(\theta)$. Then we can prove that

$$P=\frac{-i}{2\pi}\int_0^{2\pi}d\theta\,\langle\phi_0(\theta)|\,\partial_\theta\,|\phi_0(\theta)\rangle=\frac{\varphi_{\rm Z}}{2\pi}, \tag{6}$$

where $|\phi_0(\theta)\rangle$ is the ground state of $\mathcal{H}^{\rm C}_V(\theta)$, satisfying $\mathcal{H}^{\rm C}_V(\theta)\,|\phi_0(\theta)\rangle=E_0\,|\phi_0(\theta)\rangle$. The higher-order Zak phase $\varphi_{\rm Z}$ is $\mathbb{Z}_2$ quantized when the on-site potential vanishes, i.e., see Supplemental Material [76],

$$\varphi_{\rm Z}=\pi\mathbb{Z}\mod 2\pi. \tag{7}$$

On the other hand, we can demonstrate that the derivative of the polarization P with respect to time gives the current in this direction. Therefore, the amount of charge flowing through c_2 over one period is $Q_{c_2}=\int_0^{2\pi}d\tau\partial_\tau P=\Delta\varphi_{\rm Z}/2\pi$, which is related to the winding of the higher-order Zak phase

$$Q_{c_2}=\frac{-i}{2\pi}\int d\tau\int d\theta[\langle\partial_\tau\phi_0|\partial_\theta\phi_0\rangle-\langle\partial_\theta\phi_0|\partial_\tau\phi_0\rangle]. \tag{8}$$

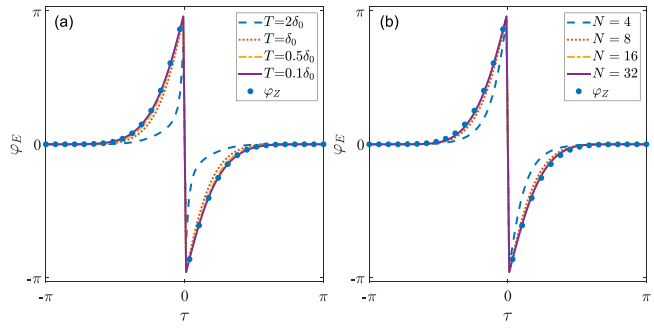

FIG. 3. (a) EGP of the HOTI at different temperatures. The system includes 10×10 unit cells. (b) EGP of the HOTI for different sizes at temperature $T = \delta_0$. The blue dots represent the higher-order Zak phase, i.e., the EGP at zero temperature.

It is equal to the Chern number, which is gauge invariant and integer quantized in a cyclic system.

Higher-order topological invariant for Gaussian mixed states. Now, we need to generalize the Zak phase and Chern number to finite-temperature scenarios. Analogous to Ref. [28], the most natural way is to generalize the ground-state expectation value of the position operator in Eq. (5) to its expectation value in the thermodynamic equilibrium state, thereby obtaining the finite-temperature Zak phase in HOTIs, i.e., the ensemble geometric phase (EGP):

$$\varphi_E = \mathrm{Im}\ln \mathrm{Tr}(\rho \hat{V}) = \mathrm{Im}\ln\langle \hat{V}\rangle. \tag{9}$$

The ground state $|\psi_0\rangle$ of $\mathcal{H}^{\mathrm{CPBC}}$ in Eq. (5) has become the equilibrium density matrix

$$\rho = \frac{1}{\mathcal{Z}}\exp(-\beta\mathcal{H}^{\mathrm{CPBC}}) = \frac{1}{\mathcal{Z}}\exp\left(-\sum_{i,j}\hat{a}_i^\dagger G_{ij}\hat{a}_j\right), \tag{10}$$

where $G = \beta\mathcal{H}^{\mathrm{CPBC}}$ is the fictitious Hamiltonian matrix, and $\beta = k_B T$ with k_B and T being the Boltzmann constant and temperature, respectively. $\mathcal{Z}$ is the partition function and $\mathrm{Tr}(\rho) = 1$.

The expectation value $\langle \hat{V}\rangle$ can be written in terms of the Gaussian integral of the Grassmann number as [28]

$$\begin{aligned}\langle \hat{V}\rangle &= \det[-f(G)]\int d(\bar{\psi},\psi)e^{\bar{\psi}[f^{-1}(G)-1+V]\psi} \\ &= \det[1-f(G)+f(G)V].\end{aligned} \tag{11}$$

Here, $\hat{a}_i^\dagger$ ($\hat{a}_i$) is replaced by the Grassmann number $\bar{\psi}$ (ψ), which satisfies the Grassmann anticommutation $\psi_i\psi_j = -\psi_j\psi_i$. V is the matrix representation of $\hat{V}$ and $f(G)$ is the correlation matrix with matrix elements

$$[f(G)]_{ij} = \langle \hat{a}_j^\dagger \hat{a}_i\rangle, \tag{12}$$

which can be analytically calculated as

$$f(G) = (e^G + 1)^{-1}. \tag{13}$$

Clearly, by definition, EGP equals the Zak phase at zero temperature. In Fig. 3(a), we have shown the higher-order EGP φ_E during a cycle at different temperatures of the same size. The blue solid dots represent the higher-order Zak phase defined in Eq. (6). We can observe that, as the temperature decreases, φ_E approaches the Zak phase φ_Z. It has been shown in Ref. [28] that for the 1D case, the EGP will reduce to the Zak phase in the thermodynamic limit, even when $T > 0$ K. We discover that this phenomenon still exists in 2D HOTI systems. Figure 3(b) illustrates the EGP at nonzero temperatures, showing that φ_E approaches the Zak phase φ_Z as the size increases.

We can define the higher-order topological invariant $\Delta\varphi_E$ at finite temperatures by calculating the winding of higher-order EGP upon a parameter loop [37], i.e.,

$$\Delta\varphi_E = \int d\tau \frac{\partial}{\partial\tau}\varphi_E = \oint_{\mathcal{P}}\left(\frac{u}{u^2+v^2}dv - \frac{v}{u^2+v^2}du\right), \tag{14}$$

where u and v are the real and imaginary parts of $\langle \hat{V}\rangle$, respectively, and $\mathcal{P}$ is the loop of $\langle \hat{V}\rangle$ in the complex plane. Since φ_E is defined modulo 2π, when the parameters return to their initial values after a cycle, the winding of φ_E must be an integer multiplied by 2π. Specifically, this integer is equal to the number of times $\langle \hat{V}\rangle$ encircles the origin in the complex plane as τ varies from 0 to 2π. At zero temperature, when the pump circle (t, Δ) contains a gapless point, i.e., the origin of the parameter space, it implies that the system is in a nontrivial topological phase. This corresponds to the loop formed by $\langle \hat{V}\rangle$ in the complex plane enclosing the origin of the complex plane. Therefore, we can examine the trajectory of $\langle \hat{V}\rangle$ in the complex plane to determine whether a topological phase transition occurs in the system as the temperature changes.

It has been pointed out that the size has no contribution to the winding of φ_E, and thus $\Delta\varphi_E$ equals the winding of the Zak phase for any size N [28]. However, our results indicate that while $\Delta\varphi_E$ is always quantized for any size, the critical

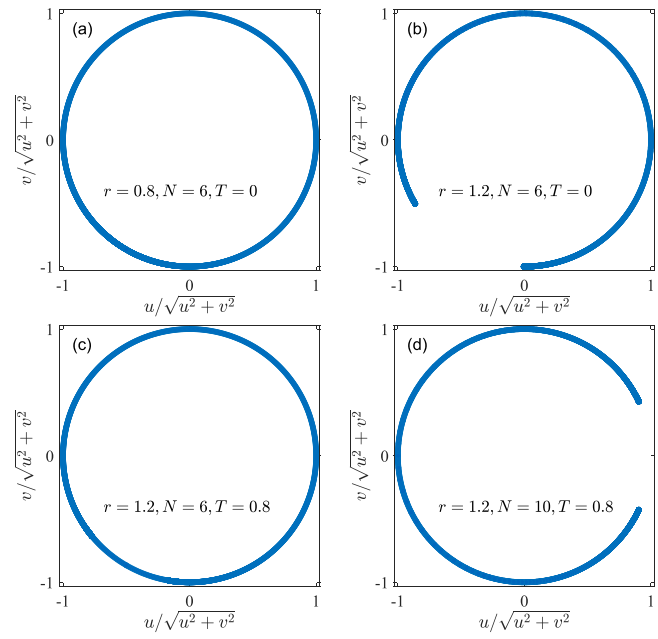

FIG. 4. The trajectory of the normalized $\langle \hat{V}\rangle$ in the complex plane when τ varies from 0 to 2π. When $T = 0$ K, the gapless point is (a) in (b) outside of the pumping circle. When $T > 0$ K and the gapless point is outside of the pumping circle, the system size is (c) $N = 6$, (d) $N = 10$.

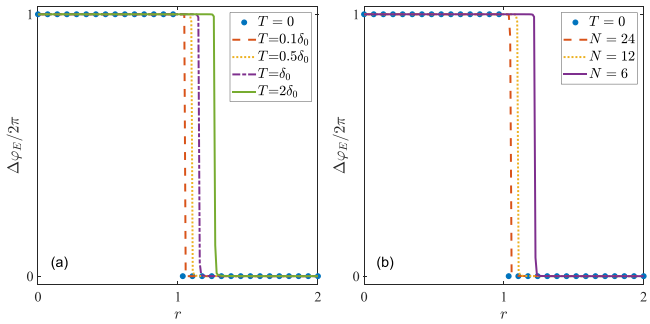

FIG. 5. (a) Difference of the higher-order EGP $\Delta\varphi_E$ accumulated per cycle vs the position of the cycle center r for different N's. The temperature of system is $T = 0.5\delta_0$. (b) $\Delta\varphi_E$ vs r for different T's. The system includes 12×12 unit cells. The trajectory of the parameters is shown in Fig. 1(b).

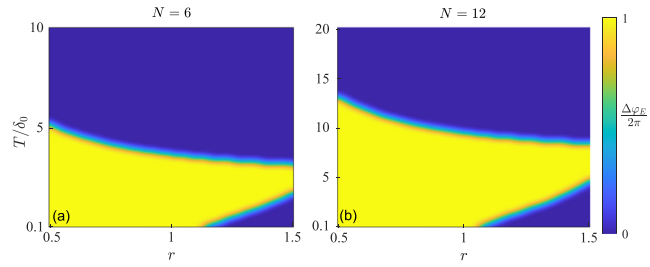

FIG. 6. Phase diagrams for the temperature T/δ_0 and r at (a) $N = 6$ and (b) $N = 12$.

point of the topological phase transition sensitively depends on N. In Fig. 4, we show the trajectory of the normalized $\langle\hat{V}\rangle$. As shown in Figs. 4(a) and 4(b), at zero temperature, when the pump circle encloses the gapless point, e.g., $r = 0.8$, the normalized $\langle\hat{V}\rangle$ forms a closed loop, corresponding to a nontrivial topological phase. However, when the gapless point is outside of the pump circle, e.g., $r = 1.2$, $\langle\hat{V}\rangle$ cannot form a closed loop, causing the system to transit to a trivial topological phase, characterized by $\Delta\varphi_E = 0$. However, when the temperature increases, as shown in Fig. 4(c), the system returns to a topologically nontrivial phase, with the normalized $\langle\hat{V}\rangle$ forming a closed loop. Interestingly, when the size is increased, as shown in Fig. 4(d), the normalized $\langle\hat{V}\rangle$ no longer forms a closed loop, indicating that in the thermodynamic limit, even at nonzero temperature, $\Delta\varphi_E$ remains consistent with $\Delta\varphi_Z$.

We show $\Delta\varphi_E$ as a function of the center of parameter circle for different sized N's in Fig. 5(a). At zero temperature, the system is in a topologically nontrivial phase when $r < 1$, in which case the pumping circle encloses the gapless point, and it is in a topologically trivial phase when $r > 1$. However, when $T > 0$, the position of the critical point will change. For a given temperature, as the size of the system increases, the critical point will approach the one at zero temperature, as shown in Fig. 5(b). It is surprising that as the temperature increases, the critical point can be greater than 1. It suggests that if the system is in a topologically trivial phase near the critical point at zero temperature, increasing the temperature will induce a topological phase transition, turning the system into a topologically nontrivial phase.

The phase diagrams are shown in Fig. 6, where the boundary between the blue (topologically trivial phase) and yellow (topologically nontrivial phase) regions represents the critical temperature as the parameter r changes. At zero temperature, the critical point of the system from the topologically nontrivial phase to the trivial phase is around $r = 1$. Due to the finite-size effects, the critical point will deviate from $r = 1$. As the temperature increases, the system transits from the topologically nontrivial phase to the trivial phase. The larger the size is, the higher the critical temperature becomes. Because according to previous theories, the EGP φ_E equals the zero-temperature Zak phase φ_Z in the thermodynamic limit, hence, the finite-temperature phase diagram approaches the zero-temperature phase diagram in the thermodynamic limit. When the system is in the topologically trivial phase as shown in Fig. 6 at zero temperature, increasing the temperature will change the system from the topologically trivial phase to the nontrivial phase, and finally back to the trivial phase.

Conclusion. In this Letter, we introduce a topological invariant for the finite-temperature states of the HOTI. The Resta's polarization at zero temperature can be generalized to the EGP at finite temperatures in the noninteracting fermionic BBH model and the winding of the EGP yields the higher-order topological invariant $\Delta\varphi_E$. The EGP defined in the higher-order topological state coincides with the higher-order Zak phase in the limit $T \to 0$. In the thermodynamic limit, i.e., $N \to \infty$, the EGPs at finite temperatures coincide with the higher-order Zak phase at zero temperature. Finite-temperature higher-order topological phases are characterized by $\Delta\varphi_E$. Our numerical simulations confirm that at finite sizes, the critical point of the topological phase transition characterized by $\Delta\varphi_E$ differs from the counterpart at zero temperature, which indicates that the temperature can induce the system to transit from a topologically trivial phase to a topologically nontrivial phase, but in the thermodynamic limit the critical points at different temperatures are the same. Our approach can be extended to 3D chiral-symmetric higher-order topological insulators. A direct method is to utilize the 3D Hamiltonian with CPBC and the 3D polarization operator proposed in Ref. [77], and use the method from this Letter to calculate the finite-temperature higher-order EGP.

Acknowledgment. This work is supported by Innovation Program for Quantum Science and Technology under Grant No. 2023ZD0300200, the National Natural Science Foundation of China under Grant No. 62461160263, Beijing Natural Science Foundation under Grant No. 1202017, and Beijing Normal University under Grant No. 2022129.

[1] X.-G. Wen, *Colloquium:* Zoo of quantum-topological phases of matter, Rev. Mod. Phys. **89**, 041004 (2017).

[2] A. Altland and M. R. Zirnbauer, Nonstandard symmetry classes in mesoscopic normal-superconducting hybrid structures, Phys. Rev. B **55**, 1142 (1997).

[3] A. P. Schnyder, S. Ryu, A. Furusaki, and A. W. W. Ludwig, Classification of topological insulators and superconductors in three spatial dimensions, Phys. Rev. B **78**, 195125 (2008).

[4] S. Ryu, A. P. Schnyder, A. Furusaki, and A. W. W. Ludwig, Topological insulators and superconductors: Tenfold way and dimensional hierarchy, New J. Phys. **12**, 065010 (2010).

[5] D. J. Thouless, M. Kohmoto, M. P. Nightingale, and M. den Nijs, Quantized Hall conductance in a two-dimensional periodic potential, Phys. Rev. Lett. **49**, 405 (1982).

[6] D. J. Thouless, Quantization of particle transport, Phys. Rev. B **27**, 6083 (1983).

[7] D. Xiao, M.-C. Chang, and Q. Niu, Berry phase effects on electronic properties, Rev. Mod. Phys. **82**, 1959 (2010).

[8] M. Z. Hasan and C. L. Kane, *Colloquium:* Topological insulators, Rev. Mod. Phys. **82**, 3045 (2010).

[9] X.-L. Qi and S.-C. Zhang, Topological insulators and superconductors, Rev. Mod. Phys. **83**, 1057 (2011).

[10] A. Uhlmann, Parallel transport and "quantum holonomy" along density operators, Rep. Math. Phys. **24**, 229 (1986).

[11] A. Rivas, O. Viyuela, and M. A. Martin-Delgado, Density-matrix Chern insulators: Finite-temperature generalization of topological insulators, Phys. Rev. B **88**, 155141 (2013).

[12] J. C. Budich and S. Diehl, Topology of density matrices, Phys. Rev. B **91**, 165140 (2015).

[13] O. Viyuela, A. Rivas, and M. A. Martin-Delgado, Uhlmann phase as a topological measure for one-dimensional fermion systems, Phys. Rev. Lett. **112**, 130401 (2014).

[14] S. Diehl, E. Rico, M. A. Baranov, and P. Zoller, Topology by dissipation in atomic quantum wires, Nat. Phys. **7**, 971 (2011).

[15] C.-E. Bardyn, M. A. Baranov, C. V. Kraus, E. Rico, A. İmamoğlu, P. Zoller, and S. Diehl, Topology by dissipation, New J. Phys. **15**, 085001 (2013).

[16] J. C. Budich, P. Zoller, and S. Diehl, Dissipative preparation of Chern insulators, Phys. Rev. A **91**, 042117 (2015).

[17] D.-J. Zhang and J. Gong, Topological characterization of one-dimensional open fermionic systems, Phys. Rev. A **98**, 052101 (2018).

[18] W. Nie, M. Antezza, Y.-X. Liu, and F. Nori, Dissipative topological phase transition with strong system-environment coupling, Phys. Rev. Lett. **127**, 250402 (2021).

[19] D. Linzner, L. Wawer, F. Grusdt, and M. Fleischhauer, Reservoir-induced Thouless pumping and symmetry-protected topological order in open quantum chains, Phys. Rev. B **94**, 201105(R) (2016).

[20] H. Wetter, M. Fleischhauer, S. Linden, and J. Schmitt, Observation of a topological edge state stabilized by dissipation, Phys. Rev. Lett. **131**, 083801 (2023).

[21] J. A. Marks, M. Schüler, J. C. Budich, and T. P. Devereaux, Correlation-assisted quantized charge pumping, Phys. Rev. B **103**, 035112 (2021).

[22] T.-S. Deng, L. Pan, Y. Chen, and H. Zhai, Stability of time-reversal symmetry protected topological phases, Phys. Rev. Lett. **127**, 086801 (2021).

[23] A. Altland, M. Fleischhauer, and S. Diehl, Symmetry classes of open fermionic quantum matter, Phys. Rev. X **11**, 021037 (2021).

[24] S. Lieu, M. McGinley, and N. R. Cooper, Tenfold way for quadratic Lindbladians, Phys. Rev. Lett. **124**, 040401 (2020).

[25] D. Paszko, D. C. Rose, M. H. Szymańska, and A. Pal, Edge modes and symmetry-protected topological states in open quantum systems, PRX Quantum **5**, 030304 (2024).

[26] Z.-M. Huang and S. Diehl, Mixed state topological order parameters for symmetry protected fermion matter, arXiv:2401.10993.

[27] R. Resta, Quantum-mechanical position operator in extended systems, Phys. Rev. Lett. **80**, 1800 (1998).

[28] C.-E. Bardyn, L. Wawer, A. Altland, M. Fleischhauer, and S. Diehl, Probing the topology of density matrices, Phys. Rev. X **8**, 011035 (2018).

[29] L. Wawer, R. Li, and M. Fleischhauer, Quantized transport induced by topology transfer between coupled one-dimensional lattice systems, Phys. Rev. A **104**, 012209 (2021).

[30] L. Wawer and M. Fleischhauer, Chern number and Berry curvature for Gaussian mixed states of fermions, Phys. Rev. B **104**, 094104 (2021).

[31] Z.-M. Huang, X.-Q. Sun, and S. Diehl, Topological gauge theory for mixed Dirac stationary states in all dimensions, Phys. Rev. B **106**, 245204 (2022).

[32] R. Unanyan, M. Kiefer-Emmanouilidis, and M. Fleischhauer, Finite-temperature topological invariant for interacting systems, Phys. Rev. Lett. **125**, 215701 (2020).

[33] Z.-M. Huang and S. Diehl, Interaction-induced topological phase transition at finite temperature, Phys. Rev. Lett. **134**, 053002 (2025).

[34] O. Balabanov, C. Ortega-Taberner, and M. Hermanns, Quantization of topological indices in critical chains at low temperatures, Phys. Rev. B **106**, 045116 (2022).

[35] L. Wawer and M. Fleischhauer, $\mathbb{Z}_2$ topological invariants for mixed states of fermions in time-reversal invariant band structures, Phys. Rev. B **104**, 214107 (2021).

[36] A. X. Pi, Y. Zhang, Y. He, and C.-C. Chien, Proxy ensemble geometric phase and proxy index of time-reversal invariant topological insulators at finite temperatures, Phys. Rev. B **105**, 085418 (2022).

[37] P. Molignini and N. R. Cooper, Topological phase transitions at finite temperature, Phys. Rev. Res. **5**, 023004 (2023).

[38] L. Mao, F. Yang, and H. Zhai, Symmetry-preserving quadratic Lindbladian and dissipation driven topological transitions in Gaussian states, Rep. Prog. Phys. **87**, 070501 (2024).

[39] F. Zhang, C. L. Kane, and E. J. Mele, Surface state magnetization and chiral edge states on topological insulators, Phys. Rev. Lett. **110**, 046404 (2013).

[40] W. A. Benalcazar, B. A. Bernevig, and T. L. Hughes, Quantized electric multipole insulators, Science **357**, 61 (2017).

[41] W. A. Benalcazar, B. A. Bernevig, and T. L. Hughes, Electric multipole moments, topological multipole moment pumping, and chiral hinge states in crystalline insulators, Phys. Rev. B **96**, 245115 (2017).

[42] J. Langbehn, Y. Peng, L. Trifunovic, F. von Oppen, and P. W. Brouwer, Reflection-symmetric second-order topological insulators and superconductors, Phys. Rev. Lett. **119**, 246401 (2017).

[43] Z. D. Song, Z. Fang, and C. Fang, $(d-2)$-dimensional edge states of rotation symmetry protected topological states, Phys. Rev. Lett. **119**, 246402 (2017).

[44] F. K. Kunst, G. van Miert, and E. J. Bergholtz, Lattice models with exactly solvable topological hinge and corner states, Phys. Rev. B **97**, 241405(R) (2018).

[45] C. W. Peterson, W. A. Benalcazar, T. L. Hughes, and G. Bahl, A quantized microwave quadrupole insulator with topologically protected corner states, Nature (London) **555**, 346 (2018).

[46] M. Serra-Garcia, V. Peri, R. Süsstrunk, O. R. Bilal, T. Larsen, L. G. Villanueva, and S. D. Huber, Observation of a phononic quadrupole topological insulator, Nature (London) **555**, 342 (2018).

[47] M. Geier, L. Trifunovic, M. Hoskam, and P. W. Brouwer, Second-order topological insulators and superconductors with an order-two crystalline symmetry, Phys. Rev. B **97**, 205135 (2018).

[48] M. Ezawa, Higher-order topological insulators and semimetals on the breathing kagome and pyrochlore lattices, Phys. Rev. Lett. **120**, 026801 (2018).

[49] F. Schindler, A. M. Cook, M. G. Vergniory, Z. J. Wang, S. S. P. Parkin, B. A. Bernevig, and T. Neupert, Higher-order topological insulators, Sci. Adv. **4**, eaat0346 (2018).

[50] X. Zhang, H. X. Wang, Z. K. Lin, Y. Tian, B. Xie, M. H. Lu, Y. F. Chen, and J. H. Jiang, Second-order topology and multidimensional topological transitions in sonic crystals, Nat. Phys. **15**, 582 (2019).

[51] X. Ni, M. Weiner, A. Alù, and A. B. Khanikaev, Observation of higher-order topological acoustic states protected by generalized chiral symmetry, Nat. Mater. **18**, 113 (2019).

[52] H. Xue, Y. Yang, F. Gao, Y. D. Chong, and B. Zhang, Acoustic higher-order topological insulator on a kagome lattice, Nat. Mater. **18**, 108 (2019).

[53] E. Khalaf, Higher-order topological insulators and superconductors protected by inversion symmetry, Phys. Rev. B **97**, 205136 (2018).

[54] F. Schindler, Z. Wang, M. G. Vergniory, A. M. Cook, A. Murani, S. Sengupta, A. Y. Kasumov, R. Deblock, S. J. I. Drozdov, H. Bouchiat, S. Guéron, A. Yazdani, B. A. Bernevig, and T. Neupert, Higher-order topology in bismuth, Nat. Phys. **14**, 918 (2018).

[55] M. J. Park, Y. Kim, G. Y. Cho, and S. B. Lee, Higher-order topological insulator in twisted bilayer graphene, Phys. Rev. Lett. **123**, 216803 (2019).

[56] Y. B. Yang, K. Li, L.-M. Duan, and Y. Xu, Type-II quadrupole topological insulators, Phys. Rev. Res. **2**, 033029 (2020).

[57] R. Chen, C. Z. Chen, J. H. Gao, B. Zhou, and D. H. Xu, Higher-order topological insulators in quasicrystals, Phys. Rev. Lett. **124**, 036803 (2020).

[58] Q. B. Zeng, Y. B. Yang, and Y. Xu, Higher-order topological insulators and semimetals in generalized Aubry-André-Harper models, Phys. Rev. B **101**, 241104(R) (2020).

[59] R. Banerjee, S. Mandal, and T. C. H. Liew, Coupling between exciton-polariton corner modes through edge states, Phys. Rev. Lett. **124**, 063901 (2020).

[60] Z. R. Liu, L. H. Hu, C. Z. Chen, B. Zhou, and D. H. Xu, Topological excitonic corner states and nodal phase in bilayer quantum spin Hall insulators, Phys. Rev. B **103**, L201115 (2021).

[61] C. B. Hua, F. Xiao, Z. R. Liu, J. H. Sun, J. H. Gao, C. Z. Chen, Q. Tong, B. Zhou, and D. H. Xu, Magnon corner states in twisted bilayer honeycomb magnets, Phys. Rev. B **107**, L020404 (2023).

[62] B. Liu, L. D. Xian, H. M. Mu, G. Zhao, Z. Liu, A. Rubio, and Z. F. Wang, Higher-order band topology in twisted moiré superlattice, Phys. Rev. Lett. **126**, 066401 (2021).

[63] R. J. Slager, L. Rademaker, J. Zaanen, and L. Balents, Impurity-bound states and Green's function zeros as local signatures of topology, Phys. Rev. B **92**, 085126 (2015).

[64] A. K. Ghosh, T. Nag, and A. Saha, Hierarchy of higher-order topological superconductors in three dimensions, Phys. Rev. B **104**, 134508 (2021).

[65] C. Wang and X. R. Wang, Disorder-induced quantum phase transitions in three-dimensional second-order topological insulators, Phys. Rev. Res. **2**, 033521 (2020).

[66] C. A. Li, B. Fu, Z. A. Hu, J. Li, and S. Q. Shen, Topological phase transitions in disordered electric quadrupole insulators, Phys. Rev. Lett. **125**, 166801 (2020).

[67] Y. B. Yang, K. Li, L. M. Duan, and Y. Xu, Higher-order topological Anderson insulators, Phys. Rev. B **103**, 085408 (2021).

[68] Y.-S. Hu, Y.-R. Ding, J. Zhang, Z.-Q. Zhang, and C.-Z. Chen, Disorder and phase diagrams of higher-order topological insulators, Phys. Rev. B **104**, 094201 (2021).

[69] C. Peng, R. Q. He, and Z. Y. Lu, Correlation effects in quadrupole insulators: A quantum Monte Carlo study, Phys. Rev. B **102**, 045110 (2020).

[70] K. Kudo, T. Yoshida, and Y. Hatsugai, Higher-order topological Mott insulators, Phys. Rev. Lett. **123**, 196402 (2019).

[71] P. L. Zhao, X. B. Qiang, H. Z. Lu, and X. C. Xie, Coulomb instabilities of a three-dimensional higher-order topological insulator, Phys. Rev. Lett. **127**, 176601 (2021).

[72] C. W. Lu, M. Zhang, H. B. Wang, Q. Ai, and T. Liu, Topological quantum transition driven by charge-phonon coupling in higher-order topological insulators, Phys. Rev. B **107**, 125118 (2023).

[73] C.-W. Lu, Z.-F. Cai, M. Zhang, H.-B. Wang, Q. Ai, and T. Liu, Effects of disorder on Thouless pumping in higher-order topological insulators, Phys. Rev. B **107**, 165403 (2023).

[74] Y. P. Wu, L. Z. Tang, G. Q. Zhang, and D. W. Zhang, Quantized topological Anderson-Thouless pump, Phys. Rev. A **106**, L051301 (2022).

[75] J. F. Wienand, F. Horn, M. Aidelsburger, J. Bibo, and F. Grusdt, Thouless pumps and bulk-boundary correspondence in higher-order symmetry-protected topological phases, Phys. Rev. Lett. **128**, 246602 (2022).

[76] See Supplemental Material at http://link.aps.org/supplemental/10.1103/PhysRevB.111.L201101 for the detailed derivations..

[77] L. Lin and C. Lee, Probing chiral-symmetric higher-order topological insulators with multipole winding number, Commun Phys **7**, 393 (2024).